7. ELECTRON POLARIMETRY

Timothy J. Gay[1]
Physics Department, University of Missouri, Rolla

7.1 Introduction

The use of electron spin as an experimental variable in studies of atomic physics provides detailed information about a variety of phenomena which is unavailable if spin is ignored. For example, analysis of the dynamics of electron exchange or tests of the importance of spin–orbit forces on continuum electrons in electron–atom collisions rely crucially on knowledge of the spins of the participating electrons. Such measurements require a source of polarized electrons, an electron polarimeter, or both. Spin experiments are being reported with increasing frequency. This is due in large part to advances over the last two decades in polarized electron technology, with regard to both sources and polarimeters. In particular, the advent of GaAs polarized electron sources and compact, efficient Mott polarimeters has dramatically lessened the difficulty associated with such experiments. These advances have led to major developments in condensed matter, nuclear, and particle physics as well as atomic physics. The physics of polarized electrons and their applications have been reviewed thoroughly in an excellent book by Kessler [1].

An ensemble of electrons is said to be spin polarized if, relative to an arbitrary axis of quantization, i, the number of electrons with spin up, $N\uparrow$, differs from that with spin down, $N\downarrow$. The degree of polarization relative to i is defined to be

$$P_i \equiv \frac{N\uparrow - N\downarrow}{N\uparrow + N\downarrow}. \tag{7.1}$$

More generally, the polarization vector is given by $\vec{\mathrm{P}} = tr[\rho\vec{\sigma}]$, where ρ is the electron ensemble's density matrix and $\vec{\sigma}$ is the Pauli spin operator. Electron polarimetry is the measurement of P_i or $\vec{\mathrm{P}}$.

Electron polarimeters can be separated roughly into two classes: those for the analysis of high-energy electrons (>1 MeV) based on electron–

---

[1] Current address: Department of Physics and Astronomy, Behlen Laboratory, University of Nebraska, Lincoln.

electron (Møller) or electron–photon scattering and those designed for analysis of relatively low-energy electrons (<1 MeV), based on Mott scattering or inelastic exchange excitation of atoms. High-energy devices are used exclusively in nuclear and particle physics experiments, whereas low-energy polarimeters are used in atomic, condensed matter, and some nuclear physics measurements. It is the latter type that we consider here.

We take the phrase "Mott scattering" to refer generally to collisions between electrons and single atoms or groups of atoms in which spin–orbit forces act on the continuum electrons, causing a left–right scattering asymmetry in the plane perpendicular to $\vec{P}$, an effect first predicted by Mott in 1929 [2]. For such an asymmetry to be appreciable, the target atoms must have high Z (>50). The scattering asymmetry A, which may be measured using the arrangement shown in Figure 1a, is defined as

$$A = \frac{N_L - N_R}{N_L + N_R}, \tag{7.2}$$

where $N_L(N_R)$ is the intensity measured at the "left" ("right") detector. The component of electron polarization perpendicular to the scattering plane defined by the detectors is given in turn by

$$P = A/S_{\text{eff}}\,(E, \theta), \tag{7.3}$$

where S_{eff}, or the "effective Sherman function," is the polarimeter's analyzing power. It depends both on the polar angle θ at which the detectors are placed and the incident electron energy E.

The dynamical cause of the Mott asymmetry is best understood by considering the semiclassical scattering potential experienced by an electron in its rest frame when scattering from a bare nucleus: $V = [(k/r) + (k'/r^3)\,M_l M_s]$. Here M_l and M_s are the orbital and spin angular-momentum projections of the continuum electron perpendicular to the scattering plane, k and k' are constants, and r is the electron–nucleus separation. For electrons with a given spin polarization, the second (spin–orbit) term of V will be positive or negative relative to the first (coulomb) term, depending on the sign of M_l. This depends in turn on whether the impact parameter of the incident electron is to the left or right of the target nucleus in the scattering plane (Figure 1b). For heavy nuclei, the spin–orbit and coulomb terms can be comparable, and the normal coulomb potential can be sufficiently modified to result in a significant left–right asymmetry.

Two reviews of Mott polarimetry have been published [3,4], and the topic is discussed in some detail in a number of other, more general reviews [5–10]. Journal articles of note, either for their overviews of the field or for their particularly detailed, careful discussions, are referenced below [11–18].

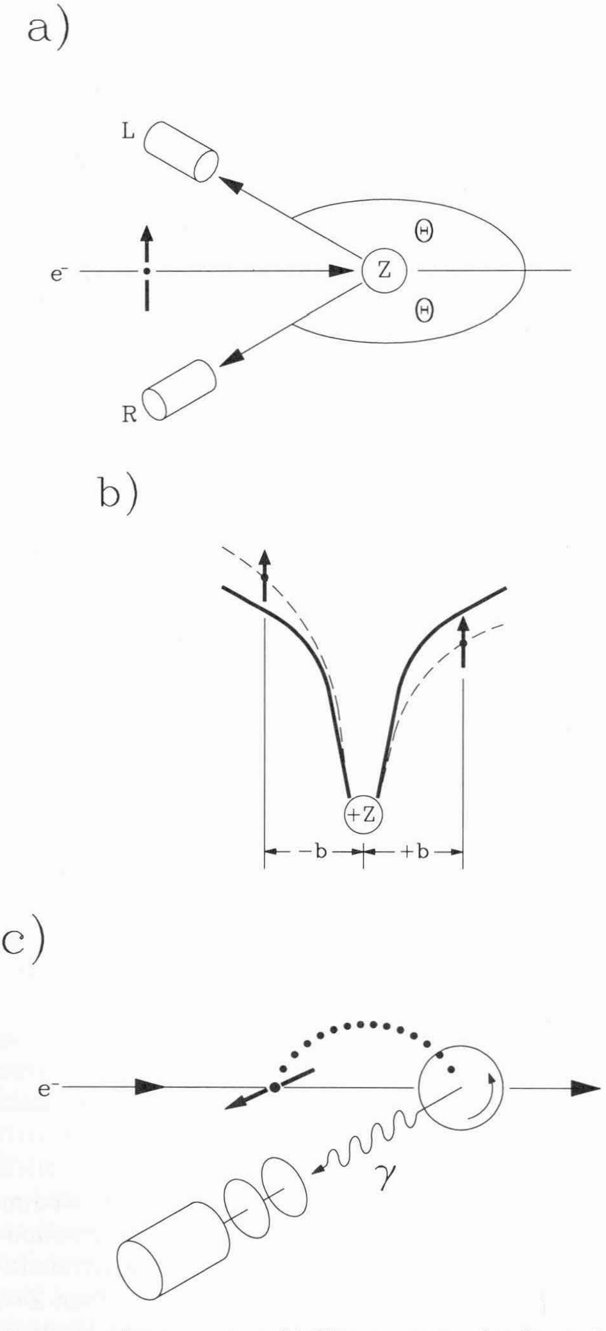

IG. 1. (a) Mott scattering geometry. (b) Electron scattering from a bare nucleus. he coulomb potential is indicated by the boldface lines; impact parameter-ependent spin–orbit perturbations are indicated by the dashed lines. (c) Geometry or optical electron polarimetry.

Optical electron polarimetry, as yet a nascent technology, involves exchange excitation of atoms by the electrons whose polarization is to be measured. In essence, the spin angular momentum of the incident electrons is converted to the oriented orbital angular momentum of the atomic excited states after the incident electrons have "taken up residence" in the atom. This conversion of spin to orbital orientation is accomplished by the spin–orbit forces active in the atom, as opposed to those acting on a scattering continuum state. The oriented atomic state will emit light with circular polariation along $\vec{P}$ when it decays (Figure 1c). In this case,

$$P = \eta_2 \Lambda, \tag{7.4}$$

where η_2 is the relative Stokes parameter associated with the circular polarization of the light and Λ, the analyzing power, is a constant dependent on the quantum numbers of the excited state. The Stokes parameter η_2 is analogous to A (Equation (7.2)) and is given by

$$\eta_2 = \frac{I^+ - I^-}{I^+ + I^-}, \tag{7.5}$$

where I^+ (I^-) is the detected intensity of light emitted along $\vec{P}$ with right (left)-handed circular polarization. Only a few reports of optical electron polarimetry in the literature exist at this time [19–23].

The choice of which polarimeter to use in a given experiment can depend on a number of often nonorthogonal factors, including cost, available space, required accuracy, incident electron flux and energy, and vacuum environment. In this chapter, we present a comprehensive review of the variety of electron polarimeters which are applicable to atomic physics experiments and consider their respective advantages and disadvantages in given situations. We also discuss techniques for the calibration of these devices and consider potential sources of error in polarimetric measurements.

7.2 Electron Polarimeters

7.2.1 The "Standard" Mott Polarimeter

The type of electron polarimeter which has been used most often in atomic physics is that of the "standard" configuration (Figure 2) [3,16,24–35]. The electrons to be analyzed are accelerated to an energy in the range 100–150 keV and then strike a thin gold (high-Z) target whose normal is parallel to the electron beam axis. Those electrons which are scattered to a polar angle of 120° in the plane perpendicular to $\vec{P}$ can strike the left and right detectors, usually of the surface-barrier type. Since the

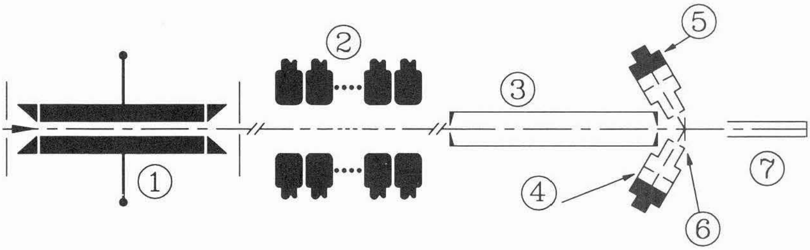

FIG. 2. The "standard" configuration for Mott polarimetry with a (1) Wien filter spin rotator. Other elements include (2) accelerator column; (3) collimator; (4) scattered-electron defining apertures; (5) surface-barrier detectors; (6) Au film target; and (7) Faraday cup.

target chamber is generally at the high-voltage end of the accelerator column, the detector signals must be transformed to ground potential.

Measuring A yields only the component of $\vec{P}$ perpendicular to the scattering plane. To measure all three components of $\vec{P}$, the vector must be rotated with some combination of electric and magnetic fields. Often Wien filters, 90° electrostatic benders, axial magnetic fields, or a combination of these are used to accomplish spin rotation prior to acceleration, where the required fields are lower. All of the components of $\vec{P}$ can be measured if the electron spins can be rotated to any direction [34]. Alternately, additional detectors can be used to determine two components of $\vec{P}$ simultaneously [25,33].

The measurement of P requires that the polarimeter's analyzing power, S_{eff}, be known. With standard polarimeters, S_{eff} is determined by measuring A for a series of target foil thicknesses, t, and using a calculated value of S, the Mott asymmetry corresponding to elastic scattering from single target atoms by electrons with $P = 1$. By extrapolating A to $t = 0$, one attains single-atom scattering conditions [35]. Calculations of S have been made for a variety of targets, electron energies, and scattering angles [36]. While detection of scattered electrons with energy resolution typical of surface barrier detectors ($\sim$10 keV) obviously does not discriminate against inelastic scattering (one assumption upon which calculations of S are based), systematic errors caused by this are small, especially at incident energies above 100 keV.

The evolution of the standard configuration is best understood by considering Figure 3. Analyzing powers with gold targets become appreciable only for angles >90° and have broad maxima in their angular dependencies between about 120° and 160°. Thus placement of the electron detectors at 120° accomplishes two things: the signal rate is maximized and the

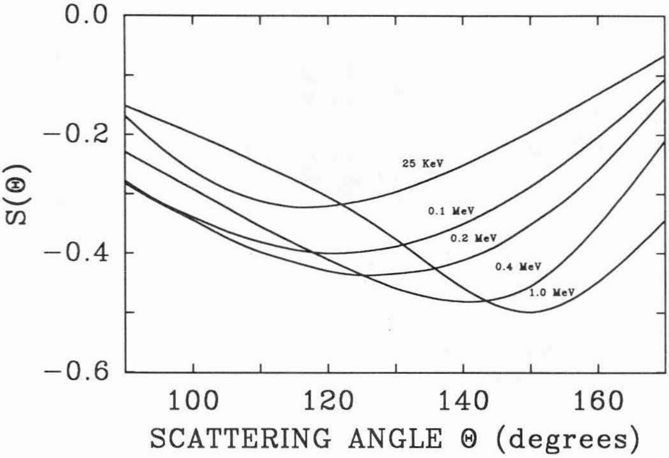

FIG. 3. Calculated values of S for Au with different values of θ and E [36].

variation of S_{eff} (or A) over the solid angles subtended by the detectors is minimized. The energy range of 100–150 keV represents a compromise between several considerations. While A increases monotonically with energy at 120° until E exceeds 1 MeV, the differential scattering cross-section decreases monotonically with energy. Moreover, multiple and plural scattering effects in the target, which reduce the accuracy with which S_{eff} can be determined, and sensitivity to target surface contamination, become increasingly bothersome as E is lowered below 100 keV.

7.2.2 The Concentric-Electrode Mott Configuration

In 1979, following a suggestion of Farago, a group at Rice University reported the design of a relatively compact Mott polarimeter which employed concentric cylindrical electrodes (Figure 4) ([14]; see also References [15,35,37]). In this configuration, a transversely polarized electron beam passes through an outer cylinder, nominally at ground potential, and is accelerated and focused by the radial field between the outer cylinder and an inner cylinder at positive high voltage between 20 and 120 kV. The beam enters a hole in the inner cylinder, where it scatters from a target foil. Electrons backscattered at 120° emerge from the inner cylinder, are decelerated by the radial field, and enter the retarding field analyzer/detectors. Those electrons that have lost too much energy in the target cannot surmount the intercylinder potential well or the potential barrier set up by the retarding fields and are thus not detected by the channel

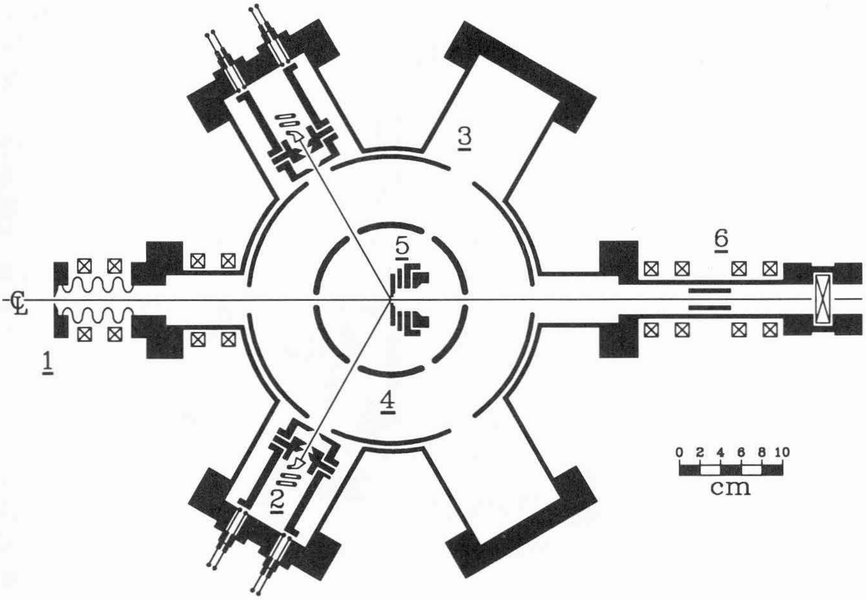

FIG. 4. Concentric-cylindrical-electrode Mott polarimeter [35]: (1) entrance aperture and input optics; (2) retarding-field analyzer/electron detector assembly; (3) grounded outer cylinder; (4) high-voltage inner cylinder; (5) movable target holder; and (6) exit electron optics.

electron multipliers (CEMs). Most of the incident electrons are scattered to angles <5° in the target and exit the polarimeter along the beam center-line.

In addition to its compactness, this design offers several advantages over standard polarimeters. Signal handling is much easier because the electrons are detected near ground potential, and the device can be used in an "in-line" orientation. Perhaps the most important advantage, though, is the good energy resolution with which the electrons are analyzed. Resolutions better than 3 eV have been reported, which essentially ensures that only elastic events are registered [35]. A foil-thickness extrapolation in conjunction with complete rejection of inelastic scattering ensures experimentally the conditions assumed in calculations of S.

To improve the efficiency and compactness of the concentric-electrode design, the Rice group has developed low-voltage devices based on spherical [23,38] and conical [39–41] (see Figure 5) geometries. These use typical inner-electrode potentials of 40 and 20 kV respectively, and are much smaller than cylindrical polarimeters; the spherical "mini-Mott" analyzer

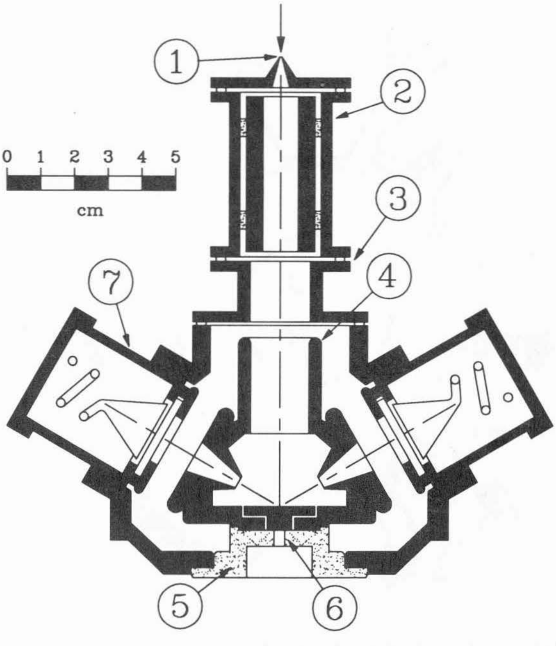

FIG. 5. Conical-electrode Mott polarimeter [39]: (1) input aperture; (2 and 3) input lenses; (4) high-voltage target assembly; (5) Macor insulator; (6) target mount; and (7) CEM housing.

has a characteristic dimension of ~15 cm while that of the conical "micro-Mott" detector is 10 cm. The CEMs in these designs subtend much larger solid angles about the beam–target interaction point than do those in the cylindrical configuration. This, in conjunction with the low operating voltages (and hence higher scattering cross sections), results in significantly higher detected electron signal for a given incident electron current.

The geometry of these smaller polarimeters permits the use of four CEMs so that two components of $\vec{P}$ can be measured simultaneously. The spherical design provides second-order focusing of the beam on the target, as opposed to the single-plane focusing of the cylindrical design. Such focusing reduces the potential for systematic error due to instrumental asymmetries (see Section 7.4.2). Focusing is provided by electrostatic lenses in the conical and standard configurations. A variant of the mini-Mott analyzer which uses cylindrical electrodes to mimic spherical fields has been developed [21]. This geometry also makes it easier to employ target-switching motion feedthroughs for foil-thickness extrapolations; the mini- and micro-Mott designs developed at Rice use single bulk-gold targets. An interesting hybrid between concentric-electrode and standard configurations, in which concentric ground and high-potential spherical electrodes provide focusing of the incident beam, while the detectors are placed in the hollow high-voltage terminal, has been reported [27].

The retarding-field analyzers used in concentric-electrode polarimeters permit the measurement of A vs ΔE, the maximum energy loss of electrons in the target. By extrapolating A to $\Delta E = 0$, one obtains the Mott asymmetry corresponding to purely elastic (albeit possibly multiple) scattering. This has been proposed as an alternative to the more difficult foil thickness extrapolation procedure. While ΔE measurements can, at high E, replace t extrapolations, care must be exercised in their application (see Section 7.4.1 and Reference [35]).

7.2.3 Atomic-Target Mott Polarimeters

While high-Z targets are required for A to be appreciable, relativistic incident electron energies are not required. Large asymmetries can also be observed with low (<1 keV)-energy electrons in elastic scattering from, e.g., single Hg atoms [7]. Polarimeters based on this principle have been in use since 1961 [42–44]. Such a device, designed for optimum efficiency and compactness, is shown in Figure 6 [17]. Transversely polarized elec-

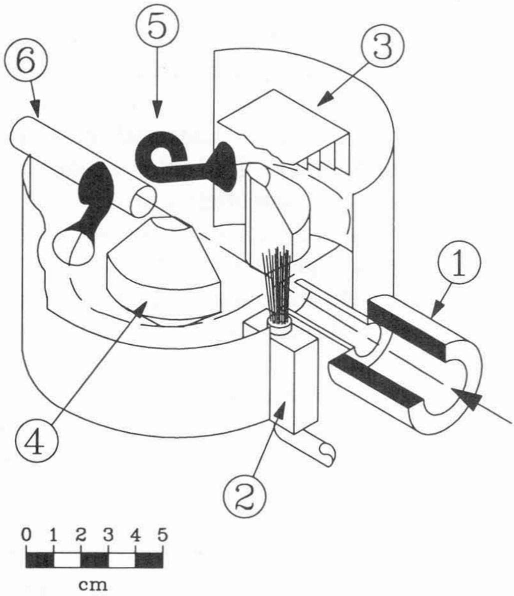

FIG. 6. Hg-vapor Mott polarimeter [17]: (1) input optics; (2) Hg vapor source; (3) L-N_2-cooled Hg trap; (4) electrostatic analyzers; (5) CEMs; and (6) Faraday cup.

trons impinge on an effusive Hg beam emerging from a heated reservoir. The Hg vapor is collected above the interaction region in a liquid-nitrogen-cooled trap. Electrons which are scattered into a fairly large solid angle centered about 90° in the plane perpendicular to $\vec{P}$ are bent in pseudospherical electrostatic analyzers and detected by CEMs. The analyzers serve three functions in this design: they shield the CEMs from UV photons generated in the interaction region, increase the detection solid angle, and provide some discrimination against inelastic scattering.

Because vapor-target densities are much lower than those associated with solid gold films, low E is a requirement for single-atom polarimeters in order to achieve reasonable efficiency. This is generally not a problem for atomic physics measurements. A notable variation in Hg vapor polarimeters is that of Gehenn [45], which has the advantage of being extremely compact and rotatable about the incident electron beam axis, so that all transverse components $\vec{P}$ can be measured with two detectors. It uses a diffuse evaporative Hg background target.

7.2.4 Low-Energy Variants with Solid Targets

A number of other polarimeters which are based on scattering asymmetries arising from an averaged nonzero spin–orbit coupling between the continuum electrons and the bulk targets have been developed. In the "diffuse scattering" Mott polarimeter (Figure 7a), the input beam (~150 eV) is focused and steered onto a vapor-deposited polycrystalline Au film target that is renewed periodically so that the device's analyzing power does not change [18,46,47]. Electrons scattered at all azimuthal angles and to polar angles between 90° and ~150° enter a collection region where they are guided by electrostatic potentials into a retarding field region, above which is placed a channelplate electron detector. The retarding field is used to discriminate against some fraction of the inelastically scattered electrons in order to maximize S_{eff}. The channelplate uses a four-segment anode to give information about both components of the transverse electron polarization.

Polarimeters based on polarized low-energy electron diffraction (PLEED) use a single-crystal target (most often W) from which the incident beam diffracts [30,48]. The left–right asymmetry of the Bragg peaks is caused by spin–orbit coupling between the crystal lattice and the incident electrons. Target surface conditions are critical, and the incident beam must have good energy and angular definition for the diffraction peaks to be resolved. While PLEED polarimeter input conditions are thus more stringent than those of diffuse-scattering polarimeters, their typical analyzing power is significantly better: ~0.3 vs 0.1.

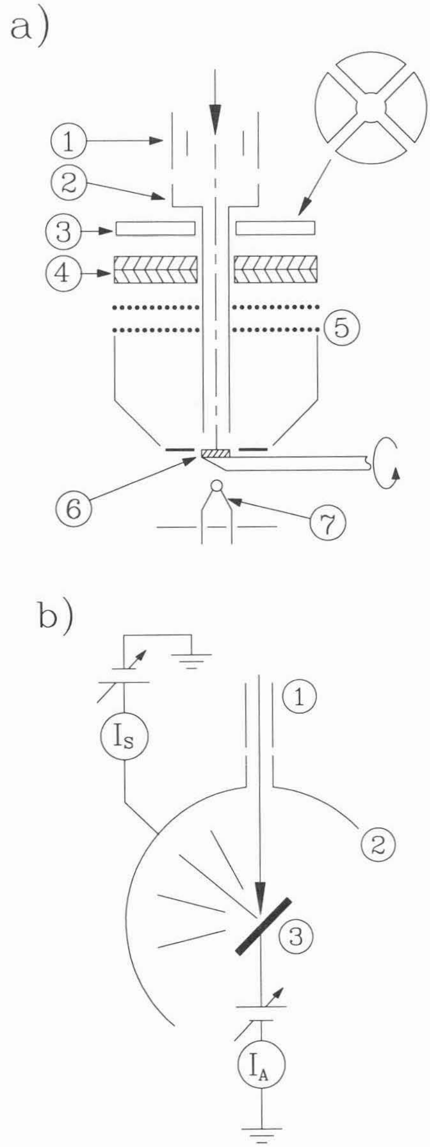

FIG. 7. (a) ''Diffuse-scattering'' low-energy Mott polarimeter [46]: (1) input optics; (2) drift tube; (3) segmented anode (see detail); (4) chevron channel plates; (5) scattered-electron extraction, guiding, and energy-discrimination electrodes; (6) target; and (7) Au evaporator. (b) ''Secondary-electron'' or ''absorbed-current'' polarimeter [52]: (1) input optics; (2) scattered/emitted current (I_s) collector; and (3) target, absorbing current I_A.

"Secondary-electron" polarimeters (Figure 7b) are based on the principle that the net current absorbed by a metallic target on which a polarized electron beam impinges is spin sensitive [48–52]. By operating at an energy (typically 160 eV for polycrystalline gold) for which the secondary electron emission from the target equals the incident current with unpolarized electrons, i.e., for which the absorbed current is zero, the absorbed current with polarized electrons will depend dramatically on P. This effect has been observed with ferromagnetic targets and with nonmagnetic crystalline and polycrystalline targets. Absorbed current polarimeters can be used only in an analog mode, but are extremely sensitive to small changes in P.

7.2.5 Optical Polarimeters

Several experiments have proven the principle of optical electron polarimetry, but no apparatuses built specifically to analyze electron polarization as an ancillary component of an experiment have been reported. Initial studies used Zn and Hg targets, but later developments involved He [20–23]. In this scheme, the ground-state target atoms are excited to the 3^3P_J multiplet, and the circular polarization η_2 of the subsequent $3^3P \rightarrow 2^3S$ florescence is measured. The electron polarization is then given by

$$P = \left(\frac{1}{2} - \frac{\eta_3}{6}\right)\eta_2 \equiv \Lambda\eta_2, \tag{7.6}$$

where η_3 is the linear polarization fraction of the light with respect to the axes parallel and perpendicular to the electron-beam axis. The incident electron energy is restricted to a range between 23.0 (threshold) and 23.6 eV to prevent cascading of higher-lying excited states into the 3^3P levels, which would invalidate Equation (7.6). In this energy range, $|\eta_3| < 0.15$, so Λ is about 0.5. Since η_3 depends only weakly on E and can be measured, an *in situ* measurement of Λ is possible.

Figure 8 shows the prototype we have used to test He for polarimetric measurements [22]. The electron beam crosses an effusive He target which is dumped into a large diffusion pump. The axis of the optical polarimeter is parallel to $\vec{\mathrm{P}}$. Light emitted along $\vec{\mathrm{P}}$ is collected and before being detected by a photomultiplier tube passes through various polarizing elements and an interference filter. Because the measurements must be made near the 3^3P excitation threshold, count rates for a given electron current are relatively low (typically 40 Hz/μA). This problem could be ameliorated by using a differentially pumped gas-cell target, as long as pressures were kept low to eliminate radiation trapping.

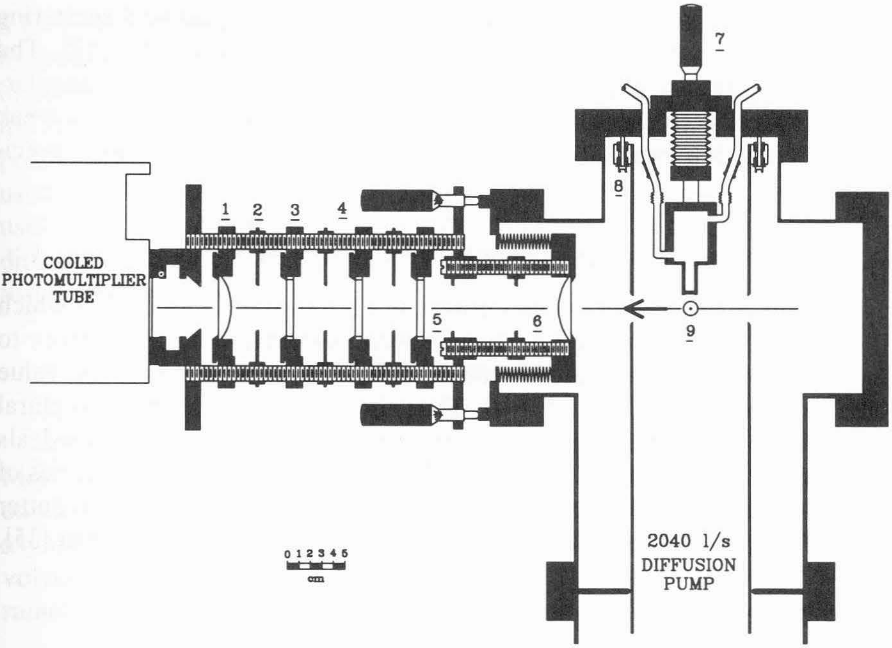

FIG. 8. He optical polarimeter [22]. Photon polarimeter elements are the (1) refocusing lens; (2) collimators; (3) interference filter; (4) linear polarizer; (5) retarder; and (6) collection lens. Also indicated are the (7) effusive gas target; (8) electrostatic target shield; and (9) electron beam (emerging from the plane of the diagram). $\vec{P}$ is indicated by an arrow.

7.3 Calibration Methods

An absolute measurement of P requires that S_{eff} or Λ be known absolutely, i.e., that the polarimeter be calibrated. There are essentially four methods for accomplishing this.

7.3.1 Calculation

If the analyzing power results from single collisions, it can be calculated directly from basic atomic scattering theory. This approach is directly applicable only to optical polarimeters and to single-atom Mott analyzers (for which S_{eff} equals S), in which the incident and scattered electron trajectories are known with confidence. Thus Hg-vapor analyzers which accept scattered electrons over a large solid angle, energy range, or both cannot be calibrated in this manner. Errors associated with calculated values of S are typical of low-energy electron–atom dynamical scattering calculations: somewhat better than 20% but worse than 2% [53]. The values of Λ, on the other hand, are determined kinematically by angular-momentum algebra and have essentially no uncertainty. There is a weak dependence of Λ on η_3, but η_3 can in turn be measured to high precision [22].

7.3.2 Asymmetry Extrapolations and Calculated S

In Mott polarimeters which allow t or ΔE extrapolations and in which the scattered electron trajectories are well characterized, S_{eff} is given to a good approximation (see Section 7.4.1) by S/A_0, where A_0 is the value of A extrapolated to t or $\Delta E = 0$. Thus the effects of multiple and plural scattering in the solid target are experimentally eliminated, and one deals in effect with single scattering. Calculations of S at the higher energies of the standard and concentric-electrode configurations are reliable to better than 5%, but the extrapolation procedure introduces additional error [35].

7.3.3 Double-Scattering Measurements

In a double-scattering measurement, unpolarized electrons scatter to a well-defined angle, θ, from a first target, thus developing a polarization $\vec{\mathrm{P}}(\theta)$ perpendicular to the scattering plane. A is determined in a subsequent, experimentally identical scattering into angles $\pm\ \theta$. Mott first suggested this experiment and showed that $A = S_{\text{eff}}^2$ [2]. This method can be used to measure the analyzing power of a Mott polarimeter directly, without resort to assumption or theoretical calculation, if a first scattering of unpolarized electrons which mimics the Mott detector's experimental geometry can be arranged. This has been done (with considerable difficulty) by several investigators to calibrate standard Mott polarimeters [12,34,42,43,54,55]. The extremely careful measurements of Gellrich *et al.* [54] represent the highest accuracy [0.3%] measurements of S_{eff} to date. A variant of the double-scattering method, involving specular diffraction of the initially unpolarized electrons from a single crystal of W, has been reported [56].

7.3.4 Use of Electrons with Known Polarization

The measurement of A with incident electrons of known $\vec{\mathrm{P}}$ yields S_{eff}. In calibrations of this type, $\vec{\mathrm{P}}$ must be measured in a preliminary experiment or produced in such a fashion that its value can be safely assumed. This has been accomplished in a variety of ways. β electrons from allowed Gamow–Teller or Fermi nuclear decays have a longitudinal polarization equal to their relativistic velocity, $\beta = v/c$, and have been used to measure

S [57]. Optical pumping of metastable He [58] and Cs [59] has been used to produce electrons with $P \approx 1$, which can then be liberated by chemi- or photoionization. In the case of He, a check on P was made by measuring the atomic polarization with a Stern–Gerlach polarimeter. Finally, optical polarimeters, which measure $\vec{P}$ to good absolute accuracy (~1%), can be used to calibrate other devices [21]. These techniques are particularly useful for the calibration of low-energy polarimeters such as the LEED, diffuse, and high-efficiency Hg vapor designs, which cannot be calibrated using other methods.

7.4 Systematic Errors

Errors in the measurements of P can arise in a number of ways. In Mott measurements, errors in the calculated value of S (if used) must be combined with uncertainties due to extrapolation procedures, instrumental asymmetries, and background signals. Optical electron polarimetry involves uncertainties related primarily to the measurement of Stokes parameters.

7.4.1 Mott Scattering: Extrapolation Errors

Because of multiple and plural scattering in solid targets, S_{eff} is less than the true atomic elastic-scattering analyzing power S. As ΔE or t increases, the discrepancy becomes larger, as shown in Figure 9. An attempt to determine S_{eff} absolutely by extrapolating A to $\Delta E = 0$ will result in error if S_{eff} for elastic scattering depends on t (curve A, Figure 9). Such errors are small (i.e., curve A is fairly flat) for $E > 100$ keV. Thickness extrapolations can lead to error if the upper bound on the range of thicknesses used is not sufficiently thin to guarantee linearity in the extrapolation form. Care must also be taken to understand the energy resolution characteristics of the RFAs used for ΔE extrapolations. Generally, errors due to extrapolation procedures are small (<5%), and decrease as E increases. These issues have been considered in detail by several authors [11,13,15,16,35].

7.4.2 Mott Scattering: Instrumental Asymmetries

Instrumental asymmetries (IAs) can be of three types: geometric, electronic, or temporal [1,3,54]. Of these, geometric IAs are most common and treacherous. Angular misalignments and/or spatial displacements of the beam on the target cause the detectors to be at different polar scattering angles and to subtend different solid angles about the beam–target inter-

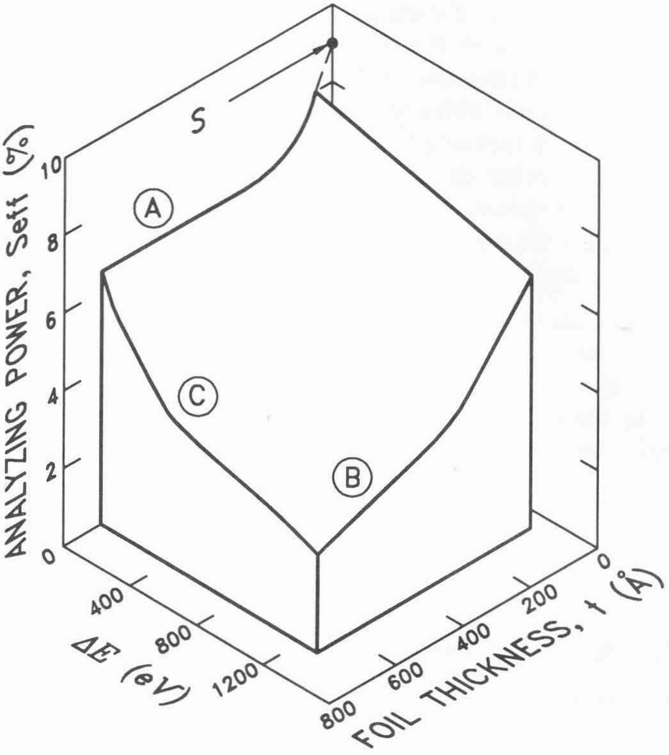

FIG. 9. Schematic representation of the effects of target thickness and electron energy loss on S_{eff} for 20-keV scattering from Au [35]. Curve B is characteristic of foil-thickness extrapolations with poor energy resolution; curve C represents a ΔE extrapolation using a bulk target (see text).

ception point. Errors in S_{eff} of ~2% per degree of angular deviation and 6% per millimeter of spatial displacement are typical. Geometric IAs could also include effects due to poorly characterized electron trajectories (due to either poor knowledge of the experimental geometry or the actions of, for example, spurious magnetic fields) that might result in misestimation of scattering angles in calculating S or S_{eff}. Monte Carlo simulation can be useful in understanding some of these effects.

Experimentally, IAs can be reduced or eliminated by the use of forward-angle monitor counters, low-Z targets for which the Mott asymmetry is small, or both; precise reversal of $\vec{P}$; the use of ZnS screens or electrodes to characterize beam positions; rotation of the entire apparatus about the incident beam axis, or a combination thereof [11,13].

Electronic asymmetries alter *A* in essentially the same way that geometric ones do, and they can be dealt with in a similar fashion. Temporal variation of *P* can also lead to errors in *A* and is most effectively reduced by frequent (and perhaps random) spin reversal.

7.4.3 Mott Scattering: Backgrounds

Background is defined as any detected signal not resulting from direct target scattering of the incident beam into the detector [1,3,11–13,16,32,55]. It can represent a significant (~20% in some cases) fraction of the total signal and is usually caused by scattering from the chamber walls or the target backing films. Three common background reduction techniques are: (1) good collimation of the incident beam and the detectors (the latter measure reduces polarimeter efficiency), (b) careful design of the electron-beam trap if it is housed in the polarimeter, and (c) chamber construction or wall coating with low-*Z* materials to minimize backscattering. In this context, an important advantage of concentric-cylinder polarimeters is their low background: the primary beam exits the chamber, eliminating the main source of backscattered electrons, and any remaining ones usually lose sufficient energy in wall collisions to be rejected by the RFAs.

7.4.4 Optical Polarimetry

The analyzing power of optical polarimeters can be determined very accurately, so uncertainty in *P* comes primarily from the photon polarimetry. With extreme care, Stokes parameters can be measured to 0.1%, but more typical uncertainties are 2–3%, due to uncertainties in the optical constants of the polarizing elements and collection lens. Procedures for the measurement of these constants are outlined in a number of references; manufacturers' claims regarding the optical properties of their wares should be regarded with caution [60]. A careful analysis of the ensemble of photon paths through the apparatus must be undertaken in the most precise work. Finally, the independence of the light polarization on target pressure must be established to eliminate the possibility of radiation trapping.

7.5 Comparison of Polarimeters

Table I compares the polarimeters discussed above. While there are no hard-and-fast rules for selecting a polarimeter for a given application, the following guidelines are generally valid. Probably the most crucial

TABLE I. Electron Polarimeters for Atomic Physics

Type	Operating energy (keV)	Required vacuum (Torr)	Size (m^3)	δ (eV)	Σ ($mm^2 \cdot sr \cdot eV$)	I/I_0	Analyzing power	Efficiency, ε	Comments	References
Mott "standard"	90–150	10^{-6}	2–10	5000	10^3	10^{-3}–10^{-2}	0.3–0.4	10^{-4}	Good efficiency without requiring external calibration; very large	3, 16, 24–35
Cylincrical concentric electrode	20–120	10^{-6}	1–2	1000	10^4	10^{-7}–10^{-6}	0.2–0.4	10^{-7}	Best for high-accuracy absolute measurements; low background; low efficiency	14, 15, 35, 37
Spherical concentric electrode	10–50	10^{-6}	10^{-1}	1000	10^4	10^{-4}–10^{-3}	0.2–0.3	10^{-5}	Compact; double focusing reduces instrumental asymmetries	21, 23, 38
Conical concentric electrode	10–35	10^{-6}	10^{-2}	500	10^3	10^{-3}	0.1–0.3	10^{-5}	Very compact	39–41
Hg beam	0.01–1	10^{-6}	10^{-2}	5	10	10^{-4}	0.1–0.4	10^{-5}	Low-efficiency versions do not require calibration; not easily UHV compatible	17, 42–44
Diffuse	0.1	10^{-9}	10^{-2}	40	10^2	10^{-2}	0.1	10^{-4}	Optimizes compactness and efficiency; requires UHV and calibration	18, 46, 47
PLEED	0.1	10^{-10}	10^{-2}	2	10	10^{-3}	0.3	10^{-4}	UHV and calibration required	30, 48
Absorbed current	0.1	10^{-9}	10^{-3}	10	1	—	—	10^{-4}	UHV and calibration required; very compact; very sensitive to changes in polarization	48–52
Optical	0.01–0.02	10^{-6}	1	0.2	10	10^{-8}	0.5–0.7	10^{-9}	Potential for best accuracy; inefficient; must be operated at low energy	20–23

requirement for a polarimeter is that it be efficient enough to measure P with reasonably small uncertainty in reasonable time. (The definition of "reasonable" being, of course, experiment dependent.) The amount of time required to measure P to a given statistical precision is inversely proportional to the "efficiency" or "figure of merit," $\varepsilon \equiv [a^2 I/I_0]^{1/2}$, where a is the device's analyzing power (either S_{eff} or Λ), I_0 is the incident beam current, and I is the detected signal rate [1]. This parameter is maximized by standard and diffuse Mott polarimeters. The efficiencies of concentric-electrode devices can be improved if Au is replaced by higher-Z targets [41,61,62]. Two related parameters are the maximum energy width of the beam, δ, that can actually be analyzed, and the electron-optical acceptance, Σ. Even if ε is large, the polarimeter is not useful if most of the beam to be analyzed is rejected by its input optics (Σ) or if the input energy range is too broad (δ) to allow a well-defined a. Sometimes the individual quantities (I/I_0) and a may be more important than their combination in ε. Experiments with extremely small values of I_0 may depend crucially on a high value of I/I_0 (the "sensitivity") alone. Beams with small P need maximal a so that systematic errors due to, for example, IAs are minimized.

Accuracy alone may be the most important requirement of an experiment. One must then pick a technique which combines good efficiency, to reduce statistical uncertainty, with good knowledge of a. For accuracy requirements of 1–2% (which is usually more than adequate in atomic physics), the cylindrical Mott analyzer is the best choice. More stringent requirements dictate the use of a double-scattering calibration or optical polarimetry.

Space, safety, cost requirements, or a combination thereof often rule out the use of a standard Mott polarimeter. If, because of beam intensity problems or transport difficulties, it is advisable to attach the analyzer directly to the experimental vacuum chamber or even place it inside an existing chamber, then use of, for example, a PLEED device may be mandatory. Vacuum requirements also play a role here. It would not be possible to use a PLEED polarimeter in most crossed-beam target chambers. Similarly, a Hg analyzer is difficult to interface directly with a UHV system. This must be kept in mind if a GaAs polarized electron source is to be used.

High-energy Mott polarimeters minimize a number of potential systematic errors, can be internally calibrated, and, in the case of the standard design, have good efficiency. Their major drawback is their size and expense. Low-energy polarimeters are small and efficient, but must ultimately be calibrated (with the exception of the optical and some Hg polarimeters). The solid target Mott devices operating below 1 keV require

UHV, are sensitive to target surface conditions, and require good control of the input beam characteristics.

A good general polarimeter which represents a nice compromise among all of the above factors is a UHV-compatible concentric-cylinder Mott analyzer run at 100 keV. With the use of low-angle monitor counters and one Al target in conjunction with a series of Au ones, it can measure P with an uncertainty associated almost entirely with the calculation of S. Its only drawback is a relatively low figure of merit.

Acknowledgment

The author acknowledges the support of the National Science Foundation.

References

1. J. Kessler, *Polarized Electrons,* 2nd ed. Springer-Verlag, Berlin, 1985.
2. N. F. Mott, *Proc. R. Soc. London, Ser. A* **124,** 425 (1929).
3. T. J. Gay and F. B. Dunning, *Rev. Sci. Intrum.* **63,** 1635 (1992).
4. D. T. Pierce, R. J. Celotta, M. H. Kelley, and J. Unguris, *Nucl. Instrum. Methods Phys. Res., Sect. A* **266,** 550 (1988).
5. P. S. Farago, *Adv. Electron. Electron Phys.* **21,** 1 (1965).
6. P. S. Farago, *Rep. Prog. Phys.* **34,** 1055 (1971).
7. J. Kessler, *Rev. Mod. Phys.* **41,** 3 (1969).
8. H. Frauenfelder and R. M. Steffan, in *Alpha, Beta, and Gamma Ray Spectroscopy* (K. Siegbahn, ed.). pp. 1431–1452. North-Holland Publ., Amsterdam, 1965.
9. H. Frauenfelder and A. Rossi, *Methods Exp. Phys.* **5B** 214–274 (1963).
10. H. F. Schopper, *Weak Interactions and Nuclear Beta Decay.* North-Holland Publ., Amsterdam, 1966.
11. A. R. Brosi, A. I. Galonsky, B. H. Ketelle, and H. B. Willard, *Nucl. Phys.* **33,** 353 (1962), and references therein.
12. J. van Klinken, *Nucl. Phys.* **75,** 161 (1966), and references therein.
13. D. M. Lazarus and J. S. Greenberg, *Phys. Rev. D* **2,** 45 (1970), and references therein.
14. L. A. Hodge, T. J. Moravec, F. B. Dunning, and G. K. Walters, *Rev. Sci. Instrum.* **50,** 5 (1979).
15. D. M. Campbell, C. Hermann, G. Lampel, and R. Owen, *J. Phys. E* **18,** 663 (1985).
16. G. D. Fletcher, T. J. Gay, and M. S. Lubell, *Phys. Rev. A* **34,** 911 (1986).
17. K. Jost, F. Kaussen, and J. Kessler, *J. Phys. E* **14,** 735 (1981).
18. See, e.g., J. Unguris, D. T. Pierce, and R. J. Celotta, *Rev. Sci. Instrum.* **57,** 1314 (1986).
19. M. Eminyan and G. Lampel, *Phys. Rev. Lett.* **45,** 1171 (1980).
20. J. Goeke, J. Kessler, and G. F. Hanne, *Phys. Rev. Lett.* **59,** 1413 (1987).
21. M. Uhrig, A. Beck, J. Goeke, F. Eschen, M. Sohn, G. F. Hanne, K. Jost, and J. Kessler, *Rev. Sci. Instrum.* **60,** 872 (1989).

22. J. E. Furst, W. M. K. P. Wijayaratna, D. H. Madison, and T. J. Gay, *Phys. Rev. A* **47,** 3775 (1993); T. J. Gay, J. E. Furst, H. Geesmann, M. A. Khakoo, D. H. Madison, W. M. K. P. Wijayaratna, and K. Bartschat, in *Correlations and Polarization in Electronic and Atomic Collisions and (e,2e) Reactions* (P. J. O. Teubner and E. Weigold, eds.), p. 265. IOP, Bristol, 1992.
23. I. Humphrey, C. Ranganathaiah, J. L. Robbins, J. F. Williams, R. A. Anderson, and W. C. Macklin, *Meas. Sci. Technol.* **3,** 884 (1992).
24. J. Kessler, J. Lorenz, H. Rempp, and W. Bühring, *Z. Phys.* **246,** 348 (1971).
25. R. Möllenkamp, W. Wübker, O. Berger, K. Jost, and J. Kessler, *J. Phys. B* **17,** 1107 (1984).
26. B. Reihl, M. Erbudak, and D. M. Campbell, *Phys. Rev. B* **19,** 6358 (1979).
27. M. Landolt, R. Allenspach, D. Mauri, *J. Appl. Phys.* **57,** 3626 (1985); M. Landolt, private communication, (1993).
28. R. Raue, H. Hopster, and E. Kisker, *Rev. Sci. Instrum.* **55,** 383 (1984).
29. M. J. Alguard, J. E. Clendenin, R. D. Ehrlich, V. W. Hughes, J. S. Ladish, M. S. Lubell, K. P. Schüler, G. Baum, W. Raith, R. H. Miller, and W. Lysenko, *Nucl. Instrum. Methods* **163,** 29 (1979).
30. M. R. O'Neill, M. Kalisvaart, F. B. Dunning, and G. K. Walters, *Phys. Rev. Lett.* **34,** 1167 (1975).
31. T. Nakanishi, K. Dohmae, S. Fukui, Y. Hayashi, I. Hirose, N. Horikawa, T. Ikoma, Y. Kamiya, M. Kurashina, and S. Okumi, *Jpn. J. Appl. Phys.* **25,** 766 (1986).
32. N. Ludwig, A. Bauch, P. Naß, E. Reichert, and W. Welker, *Z. Phys. D* **4,** 177 (1986); P. Naß, Unpublished Diplomarbeit Thesis, Universität Mainz (1982).
33. E. Kisker, G. Baum, A. H. Mahan, W. Raith, and B. Reihl, *Phys. Rev. B* **18,** 2256 (1978).
34. K. Bartschat, G. F. Hanne, and A. Wolcke, *Z. Phys. A* **304,** 89 (1982).
35. T. J. Gay, M. A. Khakoo, J. A. Brand, J. E. Furst, W. V. Meyer, W. M. K. P. Wijayaratna, and F. B. Dunning, *Rev. Sci. Instrum.* **63,** 114 (1992).
36. See, e.g., A. W. Ross and M. Fink, *Phys. Rev. A* **38,** 6055 (1988); J. W. Motz, H. Olsen, and H. W. Koch, *Rev. Mod. Phys.* **36,** 881 (1964); G. Holzwarth and H. J. Meister, *Nucl. Phys.* **59,** 56 (1964).
37. J. J. McClelland, M. R. Scheinfein, and D. T. Pierce, *Rev. Sci. Instrum.* **60,** 683 (1989).
38. L. G. Gray, M. W. Hart, F. B. Dunning, and G. K. Walters, *Rev. Sci. Instrum.* **55,** 88 (1984).
39. F. B. Dunning, L. G. Gray, J. M. Ratliff, F.-C. Tang, X. Zhang, and G. K. Walters, *Rev. Sci. Instrum.* **58,** 1706 (1987).
40. F.-C. Tang, X. Zhang, F. B. Dunning, and G. K. Walters, *Rev. Sci. Instrum.* **59,** 504 (1988).
41. D. P. Pappas and H. Hopster, *Rev. Sci. Instrum.* **60,** 3068 (1989).
42. H. Deichsel, *Z. Phys.* **164,** 156 (1961).
43. H. Deichsel and E. Reichert, *Z. Phys.* **185,** 169 (1965).
44. M. Düweke, N. Kirchner, E. Reichert, and S. Schön, *J. Phys. B* **9,** 1915 (1976).
45. W. Gehenn, R. Haug, M. Wilmers, and H. Deichsel, *Z. Angew. Phys.* **28,** 142 (1969).
46. M. R. Scheinfein, D. T. Pierce, J. Unguris, J. J. McClelland, R. J. Celotta, and M. H. Kelley, *Rev. Sci. Instrum.* **60,** 1 (1989).
47. J. Woods, M. Tobise, and R. C. O'Handley, *Rev. Sci. Instrum.* **60,** 688 (1989).

48. See, e.g., R. Feder, ed., *Polarized Electrons in Surface Physics*. World Scientific, Singapore, 1985.
49. H. C. Siegmann, D. T. Pierce, and R. J. Celotta, *Phys. Rev. Lett.* **46,** 452 (1981).
50. M. Erbudak and N. Müller, *Appl. Phys. Lett.* **38,** 575 (1981).
51. M. Erbudak and G. Ravano, *J. Appl. Phys.* **52,** 5032 (1981).
52. D. T. Pierce, S. M. Girvin, J. Unguris, and R. J. Celotta, *Rev. Sci. Instrum.* **52,** 1437 (1981), and references therein.
53. D. H. Madison, private communication (1993).
54. A. Gellrich, K. Jost, and J. Kessler, *Rev. Sci. Instrum.* **61,** 3399 (1990); A. Gellrich and J. Kessler, *Phys. Rev. A* **43,** 204 (1991).
55. P. E. Spivak, L. A. Mikaelyan, I. E. Kutikov, V. F. Apalin, I. I. Lukashevich, and G. V. Smirnov, *Sov. Phys.—JETP (Engl. Transl.)* **14,** 759 (1962), and references therein.
56. H. Hopster and D. L. Abraham, *Rev. Sci. Instrum.* **59,** 49 (1988).
57. V. Eckardt, A. Ladage, and U. V. Moellendorff, *Phys. Lett.* **13,** 53 (1964), and references therein.
58. D. M. Oro, W. H. Butler, F.-C. Tang, G. K. Walters, and F. B. Dunning, *Rev. Sci. Instrum.* **62,** 667 (1991).
59. E. H. A. Granneman, M. Klewer, and M. J. Van der Wiel, *J. Phys. B* **9,** 2819 (1976).
60. See, e.g., H. G. Berry, G. Gabrielse, and A. E. Livingston, *Appl. Opt.* **16,** 3200 (1977), and references therein.
61. R. Loth, *Z. Phys.* **203,** 66 (1967).
62. W. Eckstein, *Z. Phys.* **203,** 59 (1967).